Transactions of the TSME (2019) Vol. 7, No. 1, 45-59
Journal of Research and Applications in Mechanical Engineering

ISSN 2229-2152 print
DOI: 10.14456/jrame.2019.5

Research Article

THE CORRECTION OF THAI VARUS KNEE BY HIGH TIBIAL OSTEOTOMY WITH FUJISAWA'S POINT USING FINITE ELEMENT ANALYSIS

C. Somtua[1]
P. Aroonjarattham[1]
K. Aroonjarattham[2,*]
[1] Department of Mechanical Engineering, Faculty of Engineering, Mahidol University, 25/25, Phuttamonthol Sai 4 Rd., Salaya, Phuttamonthol, Nakornpathom 73170, Thailand
[2] Department of Orthopaedics, Faculty of Medicine, Burapha University, 169 Long-Had Bangsaen Rd., Muang District, Chonburi 20131 Thailand

Received 9 April 2019
Revised 5 June 2019
Accepted 6 June 2019

ABSTRACT:
The patients of congenital varus knees may suffer from osteoarthritis symptoms which need corrective surgery on the deformed knees. High tibial osteotomy (HTO) with Fujisawa's point is a complicated but effective treatment where the surgeon realigns the deformed varus knees to the normal knee position to preserve the ligaments, tendons and meniscus. The purpose of research was to evaluate the distributed stress and strain on the eight lower extremity models as follows: Thai varus knee, HTO corrected using Fujisawa's point varied in 5 different lateral position, 30% lateral point of load-bearing axis, 33% lateral point of load-bearing axis, 35% lateral point of load-bearing axis, 38% lateral point of load-bearing axis and 40% lateral point of load-bearing axis, HTO corrected at the midpoint of proximal tibia, and knee joint inserted with total knee prosthesis. These eight lower extremity models were evaluated under daily activities using finite element method. The stress and strain distribution of the lower extremity using HTO with Fujisawa's point were analyzed to indicate the most appropriate position to ensure that the stress and strain distribution does not exceed its maximum capacity; the femur would not break. HTO corrected using Fujisawa's point of 40% lateral point of load-bearing axis, compared to other Fujisawa's models, resulted in the maximum equivalent total strain closest to that of normal knee. However, knee joint inserted with total knee prosthesis resulted in strain distribution most similar to that of normal knee.

Keywords: *Fujisawa's point, Thai varus knee, high tibial osteotomy, finite element analysis*

1. INTRODUCTION

When the human structures bear load or motion, contact stress, wear and tear occur on human joints. There is medical evidence that the tibiofemoral joint contact pressure is related to the worsening condition of osteoarthritis and alignment of the limb [1]. The area of knee joints, medial and lateral compartment was supported the different load depending on the alignment of knee joints and activities.

Knee joint can be divided into three conditions as follows: normal alignment knees, varus knees and valgus knees [2]. First, normal alignment knees have the weight-bearing axis passing thru the femoral head to the ankle joints. Second, varus knees, which is a bow-legged deformity, is a condition of legs having an outward curvature like a

* Corresponding author: K. Aroonjarattham
E-mail address: kittaroon@gmail.com

bow in the region of knees, causing the load-bearing axis to shift to the midline of body, putting more stress and force on the medial side. The last, valgus knee is a condition of the legs having an inward curvature in the region of knees, causing the load-bearing axis to shift away from the midline of body. The conditions of knee joints are shown in Fig. 1.

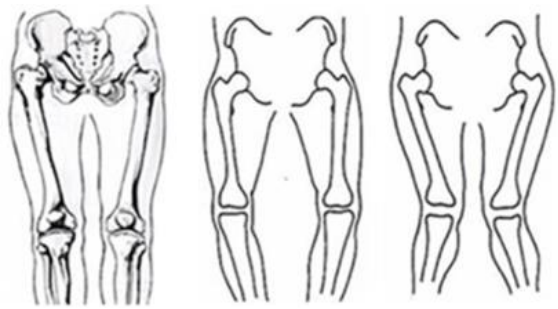

(a) (b) (c)

Fig. 1. The alignment of femur and tibia at knee joint: (a) Normal knees position, (b) Varus knees position and (c) Valgus knees position [2].

Mal-alignment knee joints cause erosion on cartilage. The corrective surgery of weight bearing axis can be performed to reduce load from the inflicted area, which is an alternative choice of knee replacement surgery. Medial compartment osteoarthritis is the most common pathology used in genu varum. There are two corrective alignment surgery choices, medial open wedge high tibial osteotomy and lateral close wedge high tibial osteotomy. However, excessive correction can decrease too much load from the medial compartment and create an overload on the lateral compartment where much pressure and progressive wear occur. The two methods to estimate load balance between medial and lateral compartment is either to set the whole mediolateral plateau to be 0 - 100% (genu varum to genu valgum) [3] or to set the midpoint to lateral to be 0 – 100% lateral and the midpoint to midial to 0 – 100% medial [4]. To correct genu varum, the mechanical axis is normally corrected to 62% width from medial to lateral tibial plateau at Fujisawa point [3], or 30% lateral [4].

The patients who have knee pain from varus knee may be diagnosed of osteoarthritis knee. Those with severe cases should be treated with Knee Arthroscopic Surgery, Total Knee Arthroplasty (TKA) or High Tibia Osteotomy (HTO) with Fujisawa's point of orthopaedic surgery [3]. The TKA surgery needs to remove some of distal femoral part and proximal tibia part of the patient to insert total knee prosthesis, which also removes part of the patients' bone, ligaments and meniscus. HTO with Fujisawa point surgery is considered an interesting treatment in this research because it adjusts the abnormal varus knee back to normal knee position by HTO with "Fujisawa point" in an effort to preserve the ligaments and meniscus. The elimination of tibia bone to change the mechanical axis from the varus to normal knee by HTO with Fujisawa point may affect the strain distribution on the lower extremity.

This research aims to evaluate the strain distribution on Thai varus knee model corrected with lateral close wedge high tibial osteotomy to change the load-bearing axis to varied Fujisawa points using finite element analysis to compare the result with Thai varus knee, Thai normal knee and knee joints with TKA surgery models to see whether the surgical treatment HTO with Fujisawa point can potentially replace total knee replacement surgery.

2. MATERIALS AND METHODS

2.1 Bone model

The bone model was constructed by reverse engineering process. Femur and tibia were scanned by the Computerized Tomography (CT) scanner and were converted into 3-D models by ITK-SNAP software to adjust the image threshold value [5, 6]. The complete model of the tight bone including Thai varus femur and tibia bone were reconstructed as shown in Fig. 2.

(a) (b)

Fig. 2. 3-D models of the tight bone: (a) Thai varus femur and (b) Thai varus tibia.

2.2 The tibial condylar plate model

The tibial condylar plate reflects an X-ray beam in the scanning process, a resin model of tibial condylar plate was used for the CT scan as shown in Fig. 3(a) and to reconstruct the three-dimensional models as shown in Fig. 3(b).

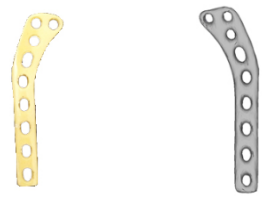

(a) (b)

Fig. 3. The tibial condylar plate: (a) Resin model and (b) 3-D model.

2.3 The screw fixation model

The screw fixation was used to fix the tibial condylar plate with the proximal tibia. 3-D model of screw fixation was created by SolidWork CAD software. The model was shown in Fig. 4 to simplify as cylinders without thread profile because the thread profile had less effect than core diameter.

Fig. 4. 3-D model of screw fixation.

2.4 The ligaments and meniscus models

Four ligaments, were secured the knee joint stability as Anterior Cruciate Ligament (ACL), Posterior Cruciate Ligament (PCL), Medial Collateral Ligament (MCL), Lateral Collateral Ligament (LCL) and the meniscus [7, 8] were created by the medical imaging program with actual anatomy position as shown in Fig. 5.

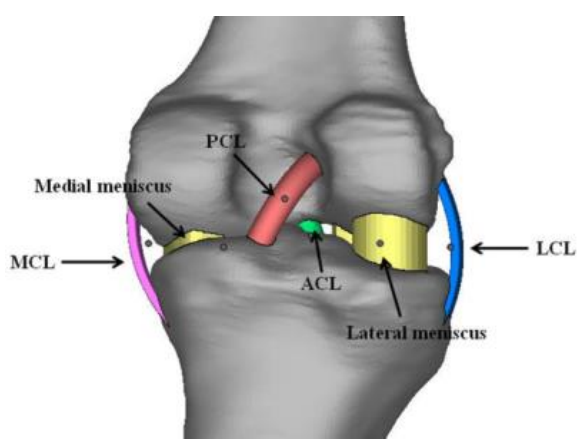

Fig. 5. 3-D models of ligaments and meniscus at knee joint.

2.5 Virtual simulations

In this research, the virtual simulation method was used to cut the proximal tibia, correct the varus knee by lateral close wedge high tibial osteotomy technique and place the fixation plate and screw to lateral tibial plateau like the actual surgery position as shown in Fig. 6.

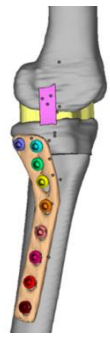

Fig. 6. 3-D models of the tibial condylar plate and screw fixation was fixing the proximal tibia.

2.6 Materials properties

Material properties of cortical bone, cancellous bone, ligaments, meniscus and implants were assumed to be homogeneous, isotropic and linear elastic. The specifications of material properties were shown in Table 1.

Table 1: Materials properties of bone, ligaments, meniscus and implants [9-11].

Material	Young's modulus (MPa)	Poisson's ratio
Cortical bone	14,000	0.30
Cancellous bone	600	0.20
Meniscus	12	0.45
Anterior cruciate ligament (ACL)	345	0.40
Posterior cruciate ligament (PCL)	345	0.40
Medial collateral ligament (MCL)	332.2	0.40
Lateral collateral ligament (LCL)	345	0.40
Tibial condylar plate	200,000	0.30
Screw fixation	200,000	0.30

2.7 Case analyses

Fujisawa's point is the point for ideal correction that shifted the axis pass through the 30% to 40% lateral side from the midpoint as shown in Fig. 7.

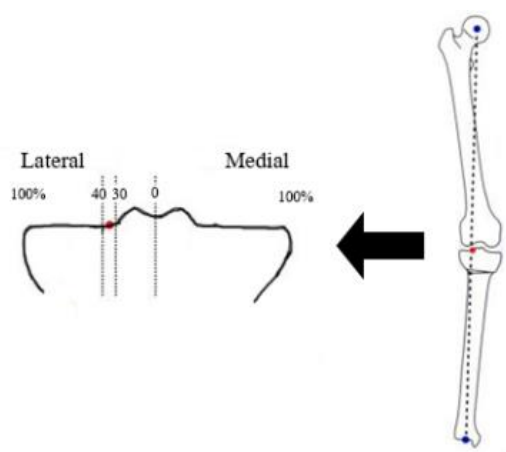

Fig. 7. Point of loading axis on the proximal tibia [4].

The cutting proximal tibia was treated by HTO to correct the load-bearing axis. The models were simulated with six cases, with varied positions of load-bearing axis as follows: the midpoint of tibial plateau (0%), 30% lateral point of load-bearing axis, 33% lateral point of load-bearing axis, 35% lateral point of load-bearing axis, 38% lateral point of load-bearing axis and 40% lateral point of load-bearing axis as shown in Fig. 8.

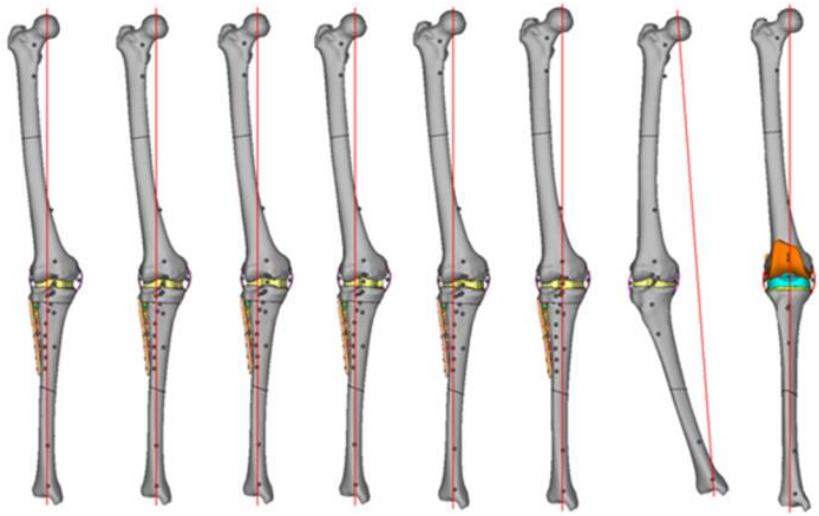

(a) (b) (c) (d) (e) (f) (g) (h)

Fig. 8. Lower extremity varied the point of weight bearing axis on tibial plateau: (a) 30% lateral point of load-bearing axis, (b) 33% lateral point of load-bearing axis, (c) 35% lateral point of load-bearing axis, (d) 38% lateral point of load-bearing axis, (e) 40% lateral point of load-bearing axis, (f) midpoint of tibial plateau and (g) varus knee and (h) total knee replacement surgery.

The line running from the femoral head through the knee joint to the center of ankle joint is called "Mikulicz line" [12]. The position of load-bearing axis was shown in Fig. 9.

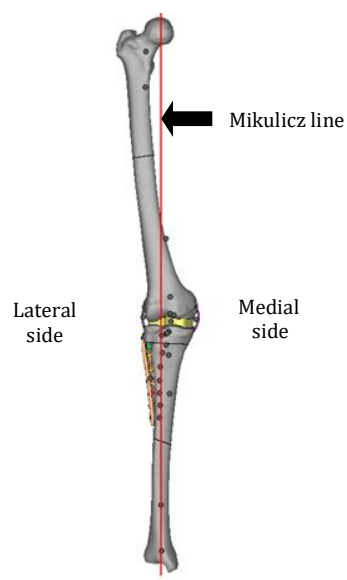

Fig. 9. Position of loading axis at 35% lateral point of load-bearing axis.

All case studies, which were analyzed by the finite element analysis (FEA) to evaluate and compare the equivalent of total strain on the medial, lateral, anterior and posterior side between the knee joint inserted total knee prosthesis, varus knee and the varus knee treated with HTO to corrected point of loading axis, were shown in Table 2.

Table 2: List of condition in the analysis.

Cases	Conditions	Point of loading axis
(a)	High tibial osteotomy	Midpoint of tibial plateau
(b)	High tibial osteotomy	30% lateral
(c)	High tibial osteotomy	33% lateral
(d)	High tibial osteotomy	35% lateral
(e)	High tibial osteotomy	38% lateral
(f)	High tibial osteotomy	40% lateral
(g)	Knee varus	-
(h)	Total knee arthroplasty	Midpoint of tibial plateau

2.8 Mesh generations

All cases were generated mesh model by MSC software package. Four-node tetrahedral element was used as a result of reducing the calculating time and similar result between the tetrahedral and hexahedral element [13]. All models were built with 4-node tetrahedral element and their mesh sizes were tested with the convergence test. The optimal mesh size used in this study was 0.8 mm [5]. The femoral bone had a total of 8,049 nodes and 29,110 elements. The tibia bone had a total of 20,948 nodes and 82,120 elements. The ligaments had a total of 7,678 nodes and 29,557 elements. The meniscus had a total of 3,577 nodes and 12,867 elements. The implants had a total of 6,565 nodes and 20,741 elements. The mesh model is shown in Fig. 10.

(a) (b) (c)

Fig. 10. Mesh model of bone-implants: (a) Femur, (b) Tibia and (c) Implants.

2.9 Boundary conditions

Boundary condition is a wrought load on the system. The force is transmitted to the femoral head due to the body weight, hip contact and muscular load on the proximal part. Two of the most common physiology activities as walking and stair-climbing condition were derived from Heller *et al.*, 2004 [14]. The tibia bone was fixed at the ankle joint. The position of force active to the bone was shown in Fig. 11 and the force magnitudes were shown in Table 3.

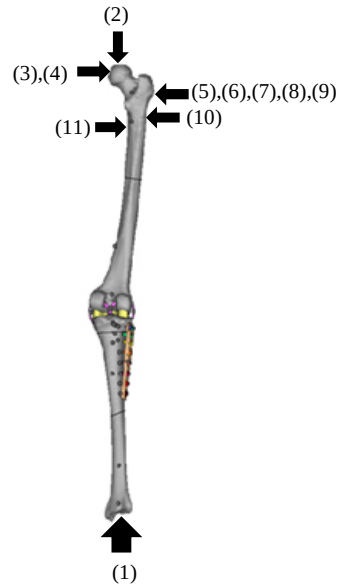

Fig. 11. The boundary condition of lower extremity.

Table 3: The load condition which applied to lower extremity [12].

Position	Force	Walking			Stair-climbing		
		F_x (N)	F_y (N)	F_z (N)	F_x (N)	F_y (N)	F_z (N)
1	Fix displacement	0	0	0	0	0	0
2	Body weight	0	0	-836.0	0	0	-847.0
3	Hip contact	-54.0	-32.8	-229.2	-59.3	-60.6	-236.3
4	Intersegmental resultant	-8.1	-12.8	-78.2	-13.0	-28.0	-70.1
5	Abductor	58.0	4.3	86.5	70.1	28.0	84.9
6	Ilio-tibial tract, proximal part	0	0	0	10.5	3.0	12.8
7	Ilio-tibial tract, distal part	0	0	0	-0.5	-0.8	-16.8
8	Tensor fascia latae, proximal part	7.2	11.6	13.2	3.1	4.9	2.9
9	Tensor fascia latae, distal part	-0.5	-0.7	-19.0	-0.2	-0.3	-6.5
10	Vastus lateralis	-0.9	18.5	-92.9	-2.2	22.4	-135.1
11	Vastus medialis	0	0	0	-8.8	39.6	-267.1

Contact conditions of MSC fragments define the relationship of the parts that are contacted. The glue contact was applied to the area where the screw fixations contact the bone that was assumed the bone ingrowths and fixed the implant rigidly and the ligaments contact the bone. The touch contact was applied to the area where the screw fixation contacts the tibial condylar plate and where femur, tibia and meniscus contact one another.

3. RESULTS

The results of FEA indicated the dispersion of equivalent of total strain on the femoral and tibia bone of eight different models under daily activities conditions.

3.1 Medial side of femoral bone

The dispersion of equivalent of total strain on the medial side of femur for all models under walking and stair-climbing conditions is shown in Figs. 12(a) and 12(b) respectively.

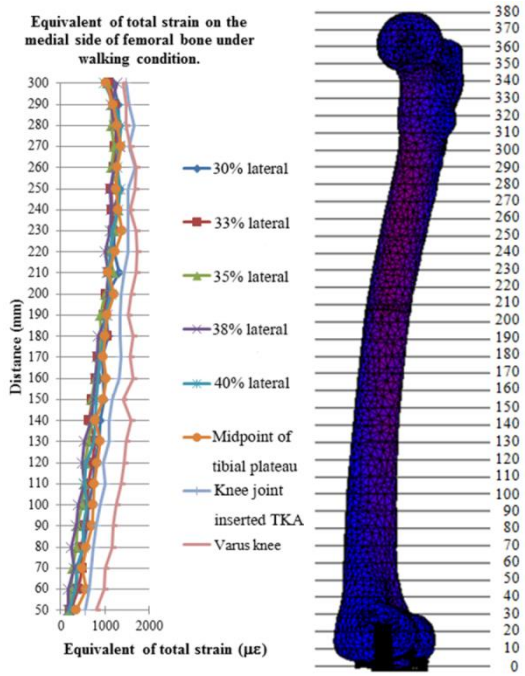

(a)

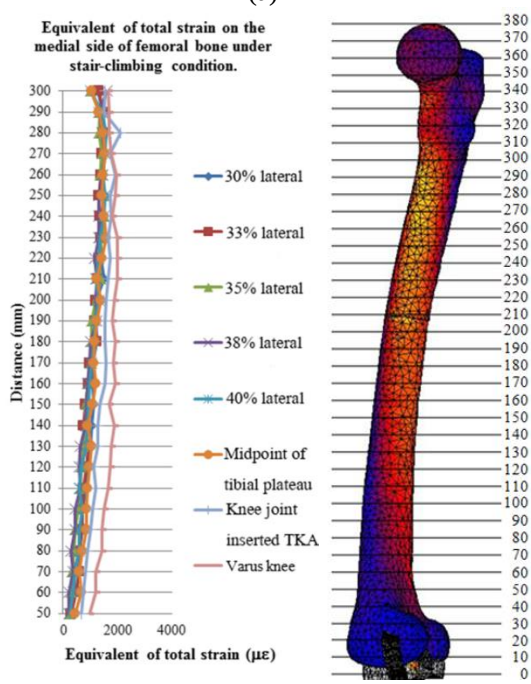

(b)

Fig. 12. The dispersion of equivalent of total strain on the medial side of femur under: (a) Walking condition and (b) Stair-climbing condition.

3.2 Lateral side of femoral bone

The dispersion of equivalent of total strain on the lateral side of femur for all models under walking and stair-climbing conditions is shown in Figs. 13(a) and 13(b) respectively.

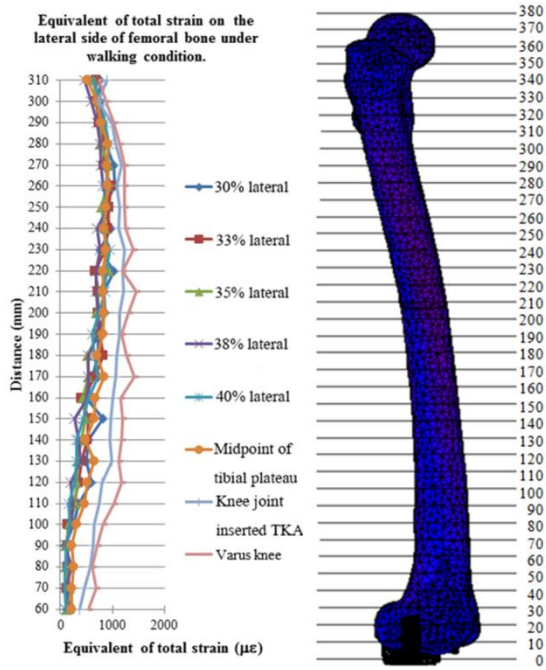

(a)

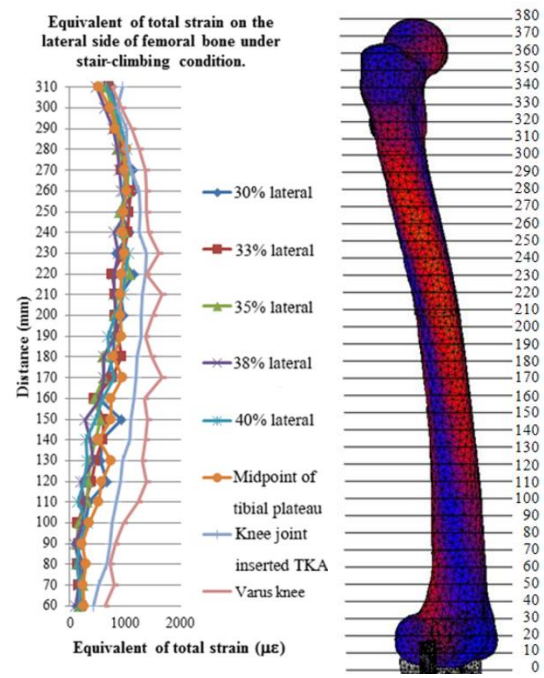

(b)

Fig. 13. The dispersion of equivalent of total strain on the lateral side of femur under: (a) Walking condition and (b) Stair-climbing condition.

3.3 Anterior side of tibia bone

The dispersion of equivalent of total strain on the anterior side of tibia for all models under walking and stair-climbing conditions is shown in Figs. 14(a) and 14(b) respectively.

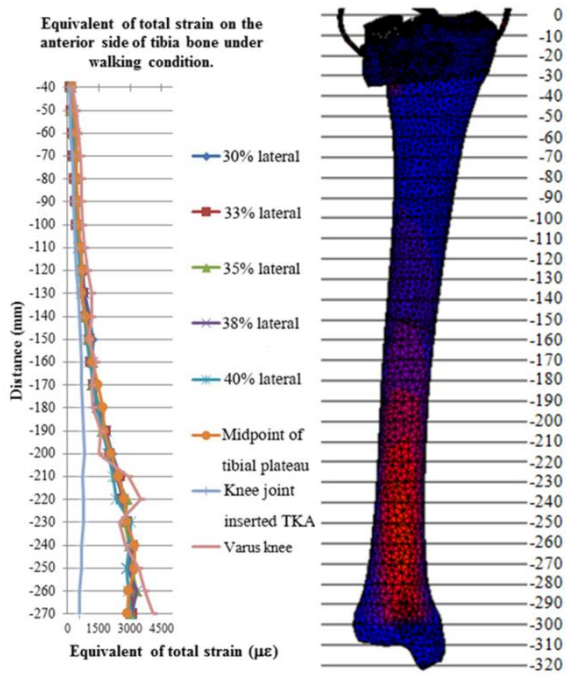

(a)

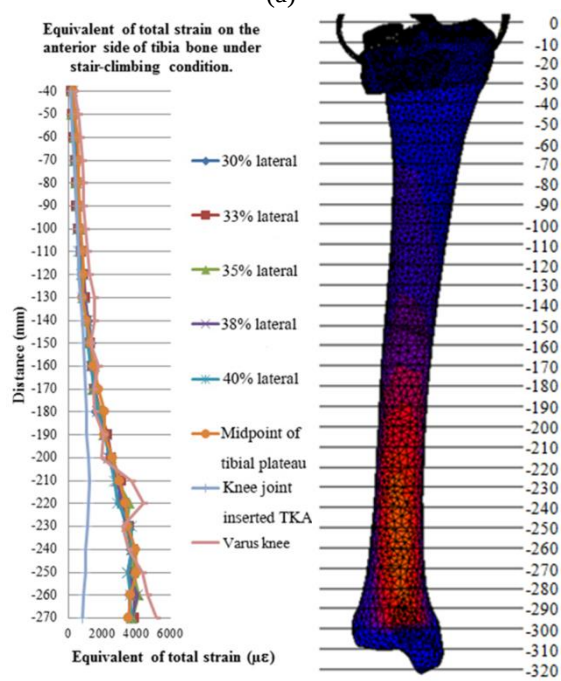

(b)

Fig. 14. The dispersion of equivalent of total strain on the anterior side of tibia under: (a) Walking condition and (b) Stair-climbing condition.

3.4 Posterior side of tibia bone

The dispersion of equivalent of total strain on the posterior side of tibia for all models under walking and stair-climbing conditions is shown in Figs. 15(a) and 15(b) respectively.

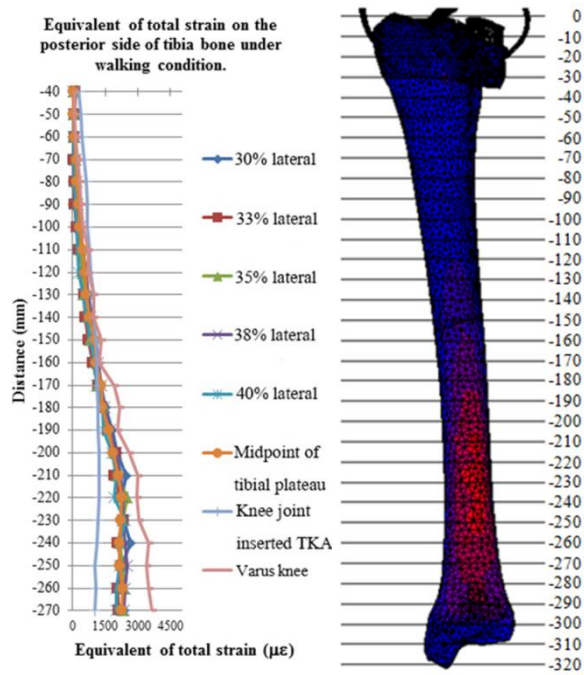

(a)

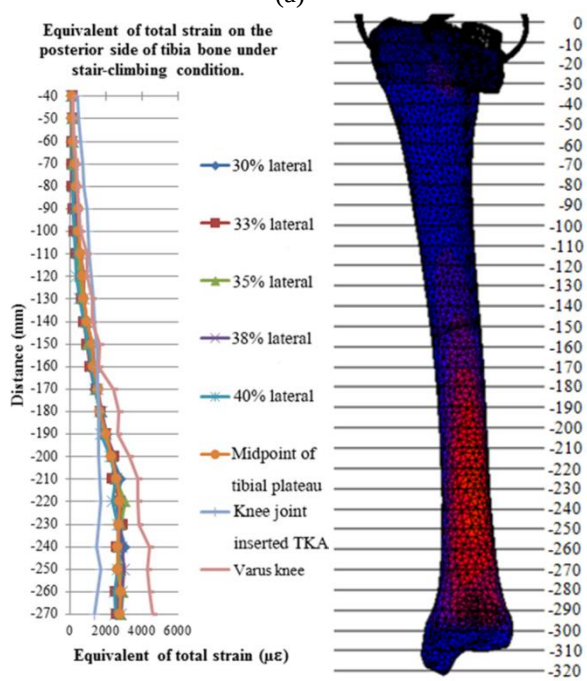

(b)

Fig. 15. The dispersion of equivalent of total strain on the posterior side of tibia under: (a) Walking condition and (b) Stair-climbing condition.

The result of varus knee correction using point of load-bearing axis as 40% lateral had the least maximum strain distribution compared to all other percentage lateral points. By using the point of 40% lateral point of load-bearing axis, the Mikulicz line was shifted closest the mechanical axis of lower extremity, resulted in its strain distribution pattern more similar to that the normal knee than any other percentage lateral points of load-bearing axis.

3.5 The tibial condylar plate

The maximum von Mises stress on the tibial condylar plate for six different models under daily activities is shown in Table 4.

Table 4: The maximum von Mises stress on the tibial condylar plate under daily activities.

Conditions	Maximum von Mises stress (MPa)	
	Walking	Stair-climbing
30% lateral	126.50	171.06
33% lateral	178.65	211.02
35% lateral	160.61	204.71
38% lateral	147.31	171.78
40% lateral	211.60	271.11
Midpoint of tibia plateau	207.94	249.44

The maximum von Mises stress on the implants did not exceed the yield strength of tibial condylar plate and screw fixation [15] that showed the implants were safe for every conditions.

4. DISCUSSION

This research was focused on analysing the strain distribution occurred on tibia bone, which was treated with HTO by cutting proximal tibia in order to correct varus knee deformity using the Fujisawa's point.

4.1 Anterior side of tibia bone

The Figs. 16 and 17 show the equivalent of total strain distribution on tibia bone at anterior side under walking and stair-climbing conditions of 4 different models: Fujisawa's point of 40% lateral point of load-bearing axis, midpoint of tibia plateau, total knee replacement and varus knee.

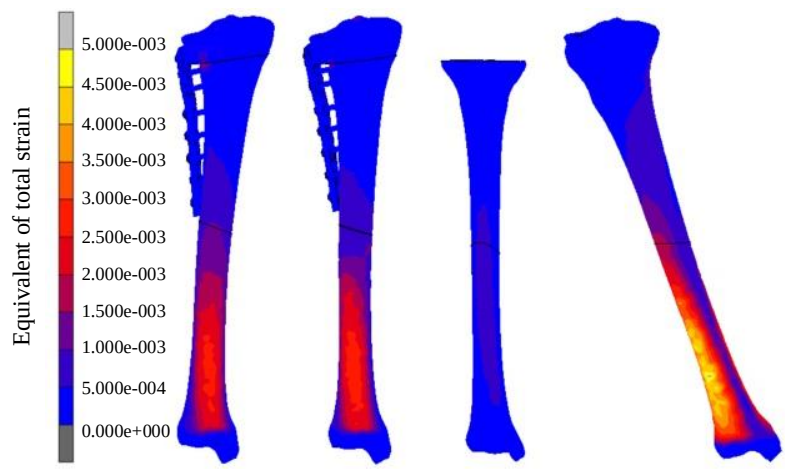

Fig. 16. The dispersion of equivalent of total strain on the anterior side of tibia bone under walking condition: (a) 40% lateral point of load-bearing axis, (b) Midpoint of tibia plateau, (c) Knee joint inserted total knee prosthesis and (d) Varus knee.

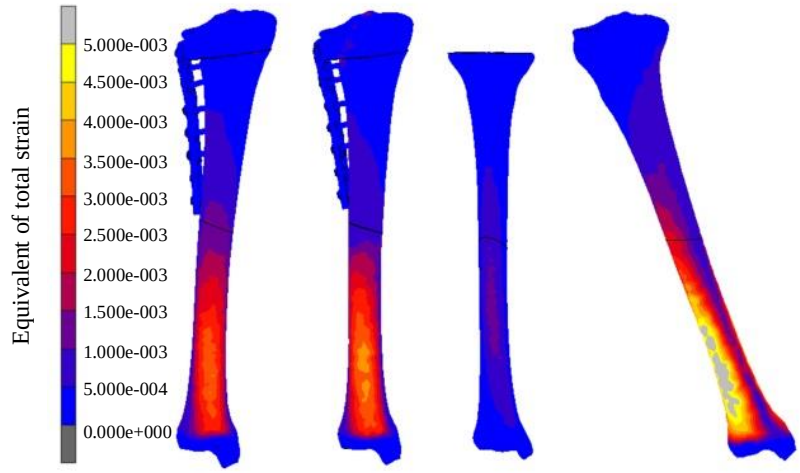

Fig. 17. The dispersion of equivalent of total strain on the anterior side of tibia bone under stair-climbing condition: (a) 40% lateral point of load-bearing axis, (b) Midpoint of tibia plateau, (c) Knee joint inserted total knee prosthesis and (d) Varus knee.

4.2 Posterior side of tibia bone

The Figs. 18 and 19 show the equivalent of total strain distribution on tibia bone at posterior side under walking and stair-climbing conditions of 4 different models: Fujisawa's point of 40% lateral point of load-bearing axis, midpoint of tibia plateau, total knee replacement and varus knee.

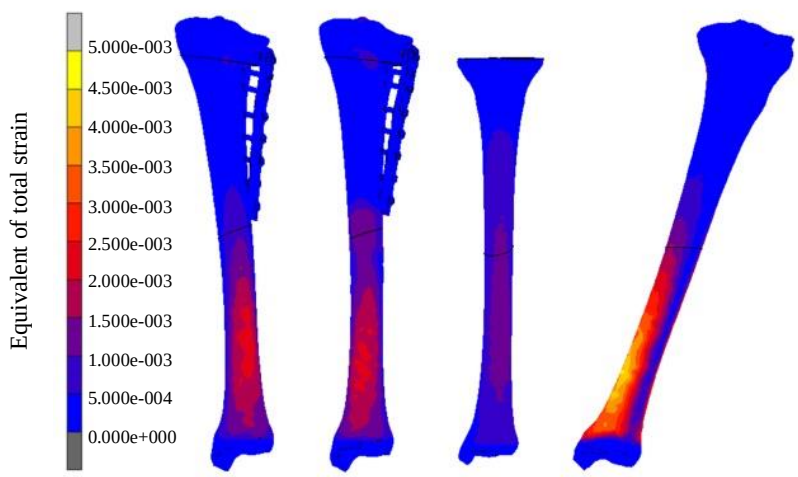

Fig. 18. The dispersion of equivalent of total strain on the posterior side of tibia bone under walking condition: (a) 40% lateral point of load-bearing axis, (b) Midpoint of tibia plateau, (c) Knee joint inserted total knee prosthesis and (d) Varus knee.

The varus knee had highest strain distribution on anterior and posterior side. Correction of varus knee using lateral close wedge HTO with 40% lateral point of load-bearing axis and midpoint of tibia plateau showed that the strain distribution decreased from the case of varus knee. Treatment of varus knee with lateral close wedge HTO with 40% lateral point of load-bearing axis and midpoint of tibia plateau can reduce the strain distribution on tibia bone because the load from femoral head can transfer through the femoral condyle to the distal tibia along the mechanical axis of lower extremity better than that of the varus model, resulting in less bending stress on tibia bone.

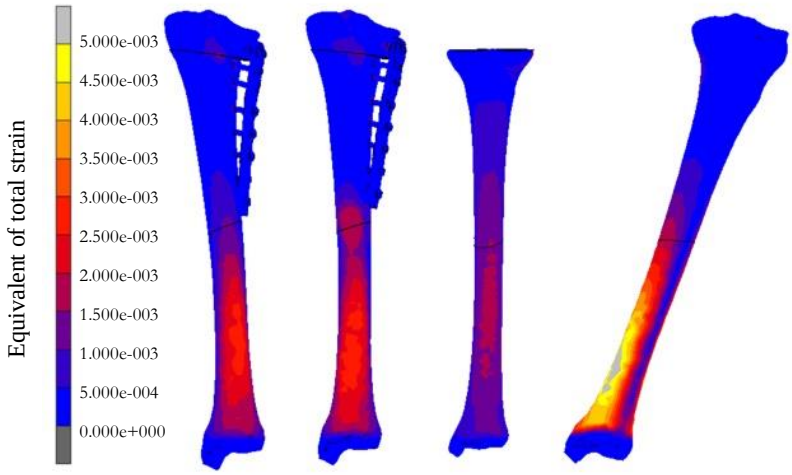

Fig. 19. The dispersion of equivalent of total strain on the posterior side of tibia bone under stair-climbing condition: (a) 40% lateral point of load-bearing axis, (b) Midpoint of tibia plateau, (c) Knee joint inserted total knee prosthesis and (d) Varus knee.

The results of FEA focused on the dispersion of strain on the femur under daily activities. The graph of Frost's mechanostat theory shows a strain magnitude greater than 25,000 microstrain on the bone with such values leading to bone fracture [16, 17].

5. Conclusion

Total knee replacement surgery adjusts femur and tibia to correct the load-bearing axis to the normal axis but HTO adjusts only tibia bone. The results compared between the 3 cases of HTO with point of loading axis 40% from lateral, HTO point of loading axis at midpoint of tibia plateau and total knee replacement surgery. The strain distribution on tibial bone from HTO loading axis 40% from lateral was less than the corrected at midpoint of tibia plateau but the least strain distribution occurred in the case of total knee replacement surgery.

Considering economical reasons, HTO is regarded as a simple, inexpensive procedure that is acceptable in many countries [18]. Michaela et al., reported the HTO patients' longevity were 94% after 5 years, 79.9% after 10 years, 65.5% after 15 years, and 54.1% after 18 years respectively [19]. HTO can be considered a suitable conduct to postpone total knee prosthesis implantation since total knee implantation in young patients can be avoided to decrease the chance of the prosthesis wearing off and possibly a repeated surgery in the future. The benefits of HTO for young patients may include wider ranges of body movement compared to that of TKA [20]. Knee joints inserted with total knee prosthesis adjusts femur and tibia to correct the bone but HTO using Fujisawa's point adjusts only tibia bone. The advantage of total knee prosthesis method is less possibility of tibia fracture while the advantage of HTO using Fujisawa's point is the preservation of ligaments, tendons and meniscus.

Acknowledgements

The authors wish to thank the Faculty of Medicine, Burapha University and Department of Mechanical Engineering, Mahidol University for their support with facilities.

References

[1] Segal, N.A., Anderson, D.D., Iyer, K.S., Baker, J., Torner, J.C., Lynch, J.A., et al. Baseline articular contact stress levels predict incident symptomatic knee osteoarthritis development in the MOST cohort, J. Orthop. Res., Vol. 27(2), 2009, pp. 1562-1568.

[2] New York-Presbyterian Morgan Stanley Children's Hospital, Bowleg and knock knees. URL: http://childrensorthopaedics.com/Bowlegand KnockKnees.html, accessed on 22/01/2013.

[3] Fujisawa, Y., Masuhara, K. and Shiomi, S. The effect of high tibial osteotomy on osteoarthritis of the knee: An arthroscopic study of 54 knee joints, Orthop. Clin. North Am., Vol. 10, 1979, pp. 585-608.
[4] Paley, D. Principles of Deformity Correction. 2002, Springer-Verlag, New York.
[5] Aroonjarattham, P., Aroonjarattham, K. and Suvanjumrat, C. Effect of mechanical axis on strain distribution after total knee replacement, J. Kasetsart (Nat. Sci.)., Vol. 48(2), 2014, pp. 263-282.
[6] Aroonjarattham, P., Aroonjarattham, K. and Chanasakulniyom, M. Biomechanical effect of filled biomaterials on distal Thai femur by finite element analysis, J. Kasetsart (Nat. Sci.)., Vol. 49(2), 2015, pp. 263-276.
[7] Knee Assessment. Inc., ©1997 Egton Medical Information Systems Limited, URL: http://www.patient.co.uk/doctor/knee-assessment, accessed on 5/05/2014.
[8] Jordan, A. The Anatomy and Function of the Knee Joint. Inc.; ©2013, URL: http://www.broadgatespinecentre.co.uk/the-anatomy-and-function-of-the-knee-joint/, accessed on 3/05/2014.
[9] Peraz, A., Mahar, A., Negus, C., Newton, P. and Impelluso, T. A computational evaluation of the effect of intramedullary nail material properties on the stabilization of simulated femoral shaft fracture, Med. Eng. Phys., Vol. 30(6), 2008, pp. 755-760.
[10] Bendjaballah, M.Z., Shiraz-Adi, A. and Zukor, D.J. Finite element analysis of human knee joint in varus-valgus, Clin. Biomech., Vol. 12, 1997, pp. 139-148.
[11] Weiss, J.A. and Gardine, J.C. Computational modeling of ligament mechanics, Crit. Rev. Biomed. Eng., Vol. 29, 2001, pp. 1-70.
[12] Monk, A.P., Van Oldenrijk, J., Nicholas, R.D., Richie, H.S.G. and Murray, D.W. Biomechanics of the lower limb, Surgery, Vol. 34(9), 2016, pp. 427-435.
[13] Ramos, A. and Simoes, J.A. Tetrahedral versus hexahedral finite elements in numerical modeling of the proximal femur, Med. Eng. Phys., Vol. 28, 2006, pp. 916-924.
[14] Heller, M.O., Bergman, G., Kassi, J.P., Claes, L., Hass, N.P. and Duda, G.N. Determination of muscle loading at the hip joint for use in pre-clinical testing, Biomechanics, Vol. 38, 2004, pp. 1155-1163.
[15] Frost, H.M. Wolff's law and bone's structural adaptation to mechanical usage: An overview for clinicians, The Angle Orthodontist, Vol. 64(3), 1994, pp. 175-188.
[16] Frost, H.M. A 2003 update of bone physiology and Wolff's law for clinicians, Angle Orthodontis, Vol. 74, 2003, pp. 3-15.
[17] Black, J. and Hastings, G. Handbook of biomaterials properties, 1998, Chapman & Hall, UK.
[18] Benzakour, T., Hefti, A., Lemseffer, M., El Ahmadi, J.D., Bouyarmane, H. and Benzakour, A. High tibial osteotomy for medial osteoarthritis of the knee: 15 years follow-up, Int. Orthop., Vol. 34, 2010, pp.209-215.
[19] Michaela, G., Florian, P., Michael, L. and Christian, B. Long-term outcome after high tibial osteotomy, Arch. Orthop. Trauma. Surg., Vol. 128, 2008, pp. 111-115.
[20] Sprenger, T.R. and Doerzbacher, J.F. Tibial osteotomy for the treatment of varus gonarthrosis, Survival and failure analysis to twenty-two years, J. Bone Joint Surg. Am., Vol. 85-A(3), 2003, pp. 469-474.